

A Comparison of Position and Rate Control for Telemanipulations with Consideration of Manipulator System Dynamics

WON S. KIM, MEMBER, IEEE, FRANK TENDICK, STUDENT MEMBER, IEEE, STEPHEN R. ELLIS, AND LAWRENCE W. STARK, FELLOW, IEEE

Abstract—Position and rate control are the two common manual control modes in teleoperations. Human operator performance using the two modes is evaluated and compared. Simulated three-axis pick-and-place operations are used as the primary task for evaluation. First, ideal position and rate control are compared by considering several factors, such as joystick gain, joystick type, display mode, task, and manipulator work space size. Then the effects of the manipulator system dynamics are investigated by varying the natural frequency and speed limit. Experimental results show that ideal position control is superior to ideal rate control, regardless of joystick type or display mode, when the manipulation work space is small or comparable to the human operator's control space. Results also show that when the manipulator system is slow, the superiority of position control disappears. Position control is recommended for small-work-space telemanipulation tasks, while rate control is recommended for slow wide-work-space telemanipulation tasks.

I. INTRODUCTION

POSITION and rate control are the two common modes for controlling remote manipulators with joysticks or hand controllers [1]–[3]. For example, the space shuttle remote manipulator system (SRMS) is provided with both position and rate control modes [4]. A small dexterous telerobotic hand which will probably be attached to the end effector of the SRMS may also be provided with both control modes [5]. Besides in space, telemanipulators have also been used in radioactive environments, underwater, and other areas.

Comparison of position and rate control performance with an Argonne National Laboratory (ANL) E2 manipulator showed that position control activated by a 1:1 replica master arm without force feedback was about four times faster in performing various tasks than resolved motion rate control activated by a six-degree-of-freedom hand controller, and about eight times faster than individual joint rate control [6], [7]. Experiments with a larger manipulator with a size ratio of 6.2:1 and a force ratio of 24:1 between the slave and master arms showed that position control with force feedback was about 1.6 times faster than resolved motion rate control [8].

The goal of our present study is to extend the previous

control mode studies by considering various factors, such as joystick gain, joystick type, display mode, task, manipulator size, and manipulator system dynamics. This study will help identify which control mode is desirable in a certain application and how it should be designed. Simulated three-axis pick-and-place operations are used as the primary task for our experiments. These simulated tasks have the advantage that experimental parameters can easily be varied over a wide range. First, ideal position and rate control modes are compared with different joystick gains, joystick types, display modes, and tasks, assuming that the manipulator system is sufficiently fast compared to human operator's control dynamics. Then the effects of manipulator system dynamics on the human operator's performance with position and rate control are investigated by performing three-axis pick-and-place tasks for various natural frequencies and also for various speed limits of the manipulator system.

II. IDEAL POSITION AND RATE CONTROL MODES

Position and rate control are the two common manual control modes for controlling telemanipulators with joysticks (or hand controllers). In position control the joystick command indicates the desired end effector position of the manipulator, whereas in rate control the joystick command indicates the desired end effector velocity.

In ideal position control, the system transfer function from the joystick displacement input to the actual manipulator hand position output $H(s)$ is a constant gain for each axis. In ideal rate control, the system transfer function is a single integrator for each axis. Namely,

$$H(s) = G_p \quad \text{for ideal position control,} \quad (1)$$

$$H(s) = G_v/s \quad \text{for ideal rate control.} \quad (2)$$

The difference equations corresponding to the continuous systems of (1) and (2) are given by

$$y(n) = G_p u(n), \quad (3)$$

$$y(n) = y(n-1) + G_v T u(n-1), \quad (4)$$

respectively, where $u(n)$ is the input, $y(n)$ the output, and T the sampling period. For our experiments with rate control, a five-percent deadband nonlinearity is introduced before the integrator to inhibit drift problems.

Manuscript received January 14, 1986; revised June 3, 1986. This work was supported in part by the Jet Propulsion Laboratory under Contract 956873 and in part by the NASA Ames Research Center, NCC 2-86 Cooperative Agreement.

W. S. Kim, F. Tendick, and L. W. Stark are with the Telerobotics Unit, 481 Minor Hall, University of California, Berkeley, CA 94720, USA.

S. R. Ellis is with the Perception and Cognition Group, ASHFD, NASA Ames Research Center, Moffett Field, CA 94035, USA.

IEEE Log Number 8715795.

A. Comparison of Ideal Position and Rate Control Modes

Three-axis pick-and-place tasks were performed with ideal position and rate control modes for various gains. Experimental methods for three-axis pick-and-place tasks are described in detail in the companion paper [9]. For convenience, a typical presentation displayed on the screen for the task is shown again in Fig. 1. The human operator controlled the manipulator hand position in robot base Cartesian coordinates by using three axes of the two displacement joysticks (Measurement Systems Model 521Z) to pick up each object with the manipulator gripper and place it in the corresponding box. Pick-and-place operations were performed sequentially from object A to D, and these four pick-and-place operations were repeated five times with different object positions for each run. Four runs from two subjects, or 80 pick-and-place operations, were performed for each experimental condition, and the corresponding mean completion time and its 90-percent confidence interval were obtained. The 90-percent confidence interval for the estimated mean based on 80 observations is given by $m \pm 1.65 s/\sqrt{80}$, where m is the mean and s is the standard deviation. Two young adult male subjects participated in the experiment. Each subject trained for at least 10 h during several days before the experiment to stabilize his performance.

Experimental results shown in Fig. 2 demonstrate that pick-and-place performance with ideal position control (2.8 s mean completion time at $G_p = 2$) was about 1.5 times faster than with ideal rate control (4.3 s at $G_v = 4$).

B. Trajectories of Joystick and Manipulator Hand Movements

To examine why position control performance was better than rate control, several trajectories of the joystick displacement input and the manipulator hand position output during pick-and-place operations were observed. Typical trajectories from the start of trying to pick up an object to its accomplishment are plotted in Fig. 3 for position, rate, and acceleration control. Only the x axis (side-to-side) component is plotted for each, since the other two axes have similar patterns. Observation of several trajectories indicates that a precise movement of the manipulator hand to a new position is achieved by a combination of quick steps and relatively slow smooth movements. Fig. 3 illustrates that in position control one quick step repositioning of the manipulator hand requires one joystick movement, whereas rate control requires a pair of opposite movements. This is a major reason why position control yields better performance than rate control for our pick-and-place tasks. It should be noted, however, that the pick-and-place task is a positioning operation. If the task is to follow a target with a constant velocity, then velocity (rate) control would perform better.

Three-axis pick-and-place tasks were also tried with acceleration control. It turned out, however, that acceleration control was not adequate to perform stable, safe pick-and-place operations (Fig. 3). In acceleration control, the manipulator tends to move virtually all the time even though the joystick is at the center position. Note that in ideal rate control,

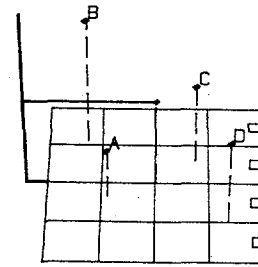


Fig. 1. Typical display presentation used for three-axis pick-and-place tasks.

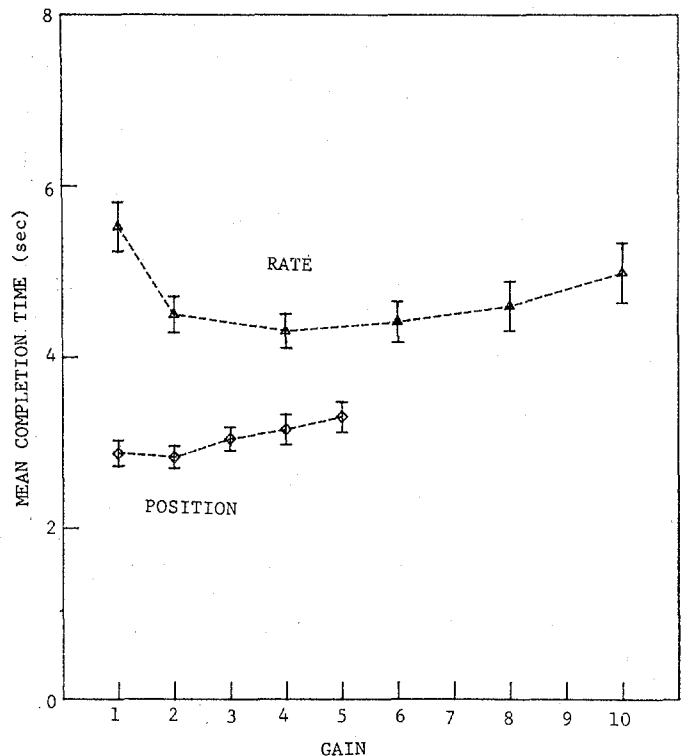


Fig. 2. Mean completion time plot for position control (\diamond) and rate control (\triangle) with various gains. Vertical bar indicates 90 percent confidence interval for mean.

the manipulator does not move when the joystick is at the center position regardless of previous history of joystick displacement. Difficulty in using acceleration control is also briefly mentioned in [10].

C. Effects of Gain Change

Fig. 2 shows that the mean completion time did not change much for the various gains tested, which means that the human operator adapted well to the gain change. This result is consistent with previous manual tracking experiments demonstrating the human operator's remarkable adaptation capabilities [11], [12]. In Fig. 2, both lower and higher gains relative to the optimal gains caused slight increase in the mean completion time. A reason for slightly longer mean completion times with lower gains is that lower gains demand wider joystick displacements. A reason for slightly longer mean completion times with higher gains is that higher gains demand more minute joystick displacements, degrading effective resolution of the joystick control. An additional major reason for longer mean completion times with lower gains for the rate

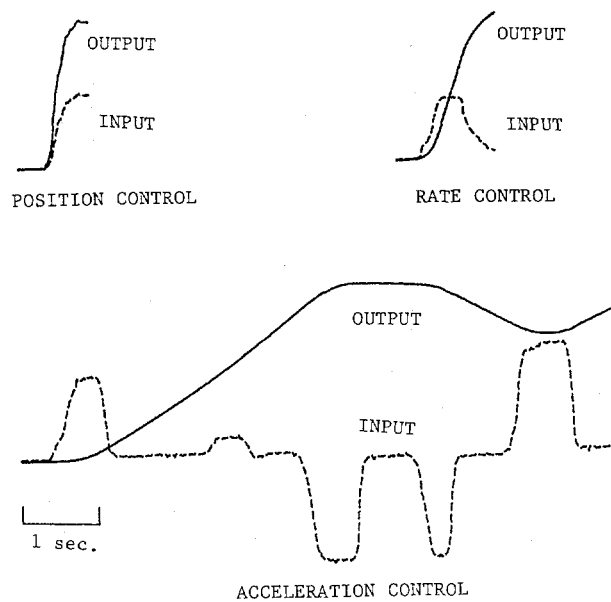


Fig. 3. Trajectories of joystick control input (---) and manipulator hand position output (—) for position, rate, and acceleration control.

control is due to the velocity limit, which will be further investigated in Section III-C.

D. Force Joystick

There are two common joystick types: the displacement joystick whose output is proportional to the joystick displacement, and the force (isometric or stiff) joystick whose output is proportional to the force applied by the human operator. The advantage of the force joystick is that it requires only minute displacements (a few microns) compared to the displacement joystick (a few centimeters).

Two-axis pick-and-place tasks were performed for ideal position and rate control with a displacement joystick (Measurement Systems Model 521Z) and a force joystick (Measurement Systems Model 404). Two-axis pick-and-place tasks will be described in the next section. Joystick gains were set at $G_p = 2$ for position control and $G_v = 4$ for the two rate controls, since these gains showed the lowest mean completion times in Fig. 2. The results for two subjects show that in the rate control mode, performance with the force joystick was faster than with the displacement joystick (Fig. 4). This is because the force joystick senses the applied force directly, requiring only very minute joystick displacements. In the position control mode, however, the force joystick performed no better than the displacement joystick. In fact, both subjects preferred to use the displacement joystick in this mode, since the force joystick required more force to be applied than the displacement joystick, especially when the manipulator hand was to be positioned far away from the initial center position. Fig. 4 also demonstrates that position control performance was better than rate control regardless of joystick type.

E. Two Display Modes

So far we have assumed that the camera is fixed with respect to the manipulator base, and the manipulator hand on the display moves in accordance with the actual manipulator hand

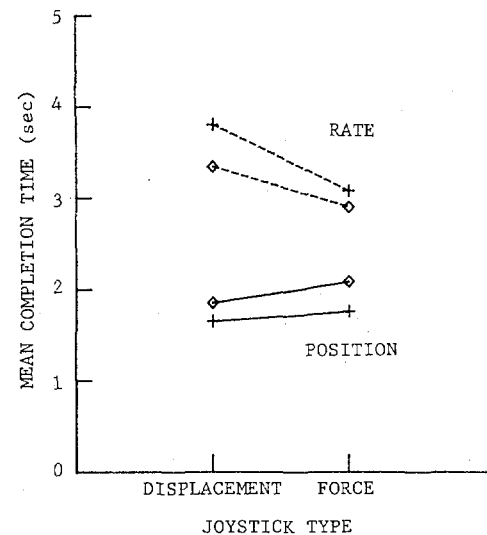


Fig. 4. Effects of joystick type on performance of position control (—) and rate control (---). Two subjects: WK (◇), MT (+).

movement. This camera-at-base mode corresponds to the pursuit (outside-in) display mode [13], [14]. However, when the camera is mounted on the manipulator forearm and directed towards the manipulator hand, the hand is fixed on the display even when the hand moves. Instead, the background scene moves on the display in the opposite direction of the manipulator arm movement. This camera-at-forearm mode corresponds to the compensatory (inside-out) display mode. The camera-at-forearm mode often provides better viewing with more magnification and probably less occlusion as compared with the camera-at-base mode. However, in our experiment, both display modes were assumed to have the same viewing condition except that they used different reference frames for the display.

To investigate the effects of the two display modes, two-axis pick-and-place tasks were performed with ideal position and rate controls for both display modes. A typical example of initial display patterns is shown in Fig. 5. Joystick gains were set at $G_p = 2$ and $G_v = 4$ as before. Fig. 6 shows the mean completion time results for two subjects. Each subject performed 100 pick-and-place operations for each condition. The results show that position control yielded better performance than rate control regardless of the display mode. The results also show that the pursuit display mode yielded better performance than the compensatory display mode for both position and rate control. This result can be understood by considering that in the compensatory display mode, the background scene moves in the opposite direction of the joystick displacement, while in the pursuit display mode, the manipulator hand moves in accordance with the joystick displacement. The two display modes considered here with pick-and-place tasks are similar to the two display modes which will be considered next with manual tracking tasks.

F. Single-Axis Tracking Task

Single-axis tracking tasks with both pursuit and compensatory modes [11], [15]–[17] were performed with position and rate control to test the generality of our results obtained with

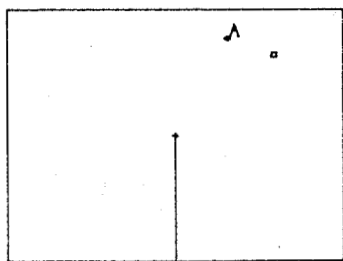


Fig. 5. Typical presentation for two-axis pick-and-place tasks.

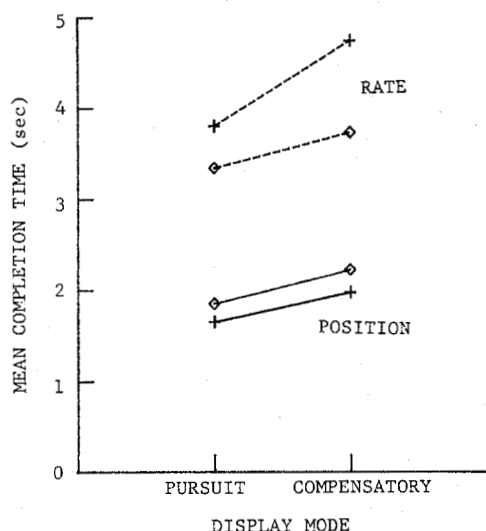


Fig. 6. Mean completion time plot for position control (—) and rate control (---) with two display modes. Subjects: WK (◇), FT (+).

pick-and-place tasks. In the pursuit mode, both target position and the system output position were indicated on the display. In the compensatory mode, only the position error between the target and the output was indicated. The human operator controlled the system output position with a displacement joystick to follow the target or to reduce the error between the target and the output. The transfer function from the joystick input to the system output position was G_p for position control, and G_v/s for rate control. Joystick gains were set at $G_p = 2$ and $G_v = 4$ as in the previous pick-and-place tasks.

Two subjects performed tracking tasks. Each subject used five different target trajectories for each condition. Each trajectory was constructed by the summation of ten sinusoids of 0.05, 0.1, 0.2, 0.35, 0.55, 0.9, 1.65, 2.2, 3.15, and 4.15 Hz. The magnitude of each sinusoid was chosen so that the magnitude spectrum of the target appeared to be that of a first-order low-pass filter with cutoff frequency of 0.1 Hz. The phase of each sinusoid was randomly chosen. Different trajectories were obtained by selecting different phase values. Each tracking task lasted 50 s, of which the first 10 s were warmup. Tracking performance was evaluated in both time and frequency domains. Root-mean-squared (rms) tracking error was used as the performance measure for the time domain analysis. Bode plots were used for the frequency domain analysis.

Normalized rms tracking error results are plotted in Fig. 7. This rms error plot is very similar to the mean completion time plot of Fig. 6 obtained from pick-and-place tasks. That is,

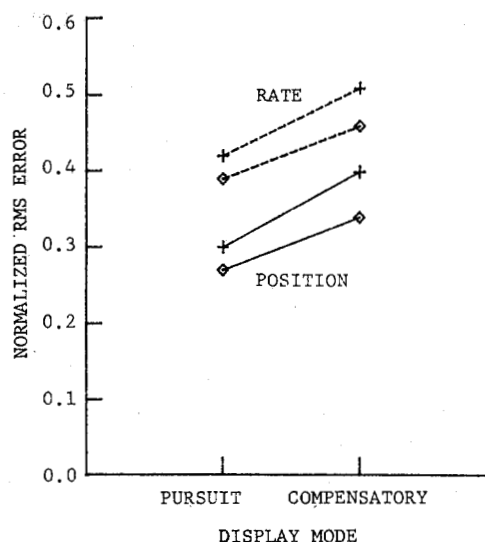


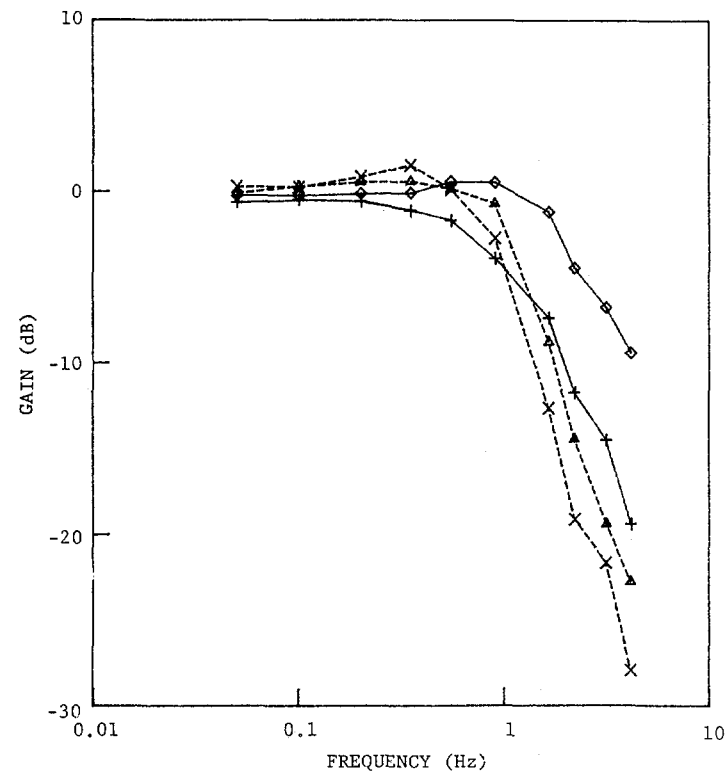
Fig. 7. Normalized rms error plot for position control (—) and rate control (---) with two display modes. Subjects: WK (◇), FT (+).

position control yielded better performance than rate control, and the pursuit display mode yielded better performance than the compensatory mode. These results are consistent with previous manual tracking experimental results [14].

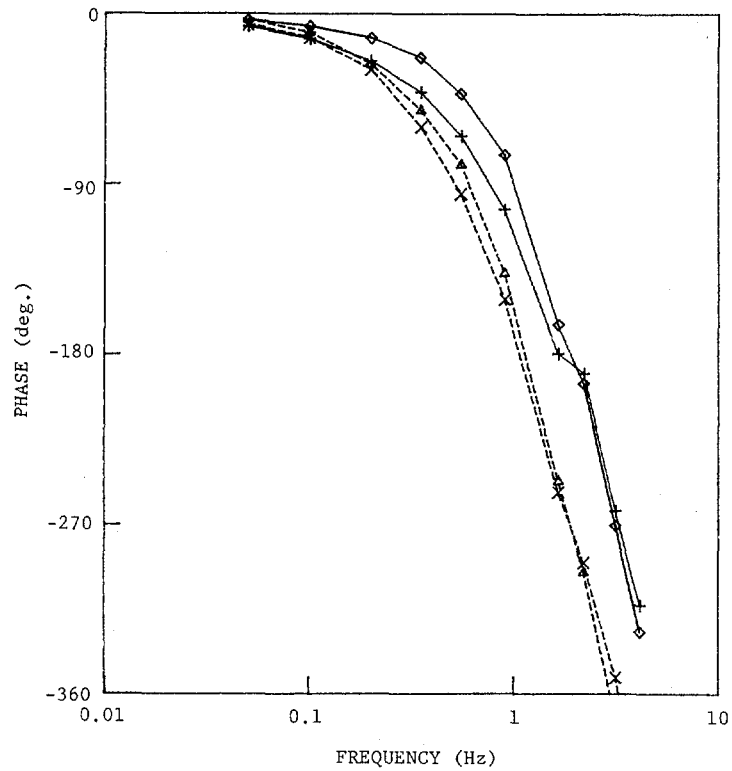
Bode plots of the closed-loop transfer function between the target input $r(t)$ and the human-operator-controlled system output $y(t)$ are shown in Fig. 8 for both control modes and both display modes. The Bode plots of the open-loop transfer function between the position error $r(t) - y(t)$ and the system output $y(t)$ are shown in Fig. 9. For pursuit tracking, the open-loop transfer function includes the effect of a target position feedforward path. Each of these Bode plots was obtained by averaging ten individual Bode plots from two subjects. Figs. 8 and 9 show that pursuit tracking has wider bandwidth and/or better phase response than compensatory, and also show that position control has wider bandwidth and/or better phase response than rate control.

G. Resolution

All the foregoing experimental results demonstrate the superiority of ideal position control. However, our pick-and-place task (Fig. 1) implicitly assumed that the manipulator work space was small or comparable to the joystick control space by allowing the task to be performed with a display showing the entire manipulator work space in one screen. Note that if the size of the manipulator were very large like the SRMS, most pick-and-place operations of practical interest would require an enlarged partial display for successful performance. Examples of small-work-space manipulators are nuclear reactor teleoperators, surgical micromanipulators, and a small dexterous telerobotic hand attached to the end of the main manipulator. Position control can also be utilized during proximity operations in conjunction with force-reflecting joysticks for enhanced telepresence [18]. When the telemanipulator's work space is very large, position control suffers from poor control resolution, since the human operator's control movements must be greatly amplified to allow the telemanipulator's full range of motion [19]. One way to solve

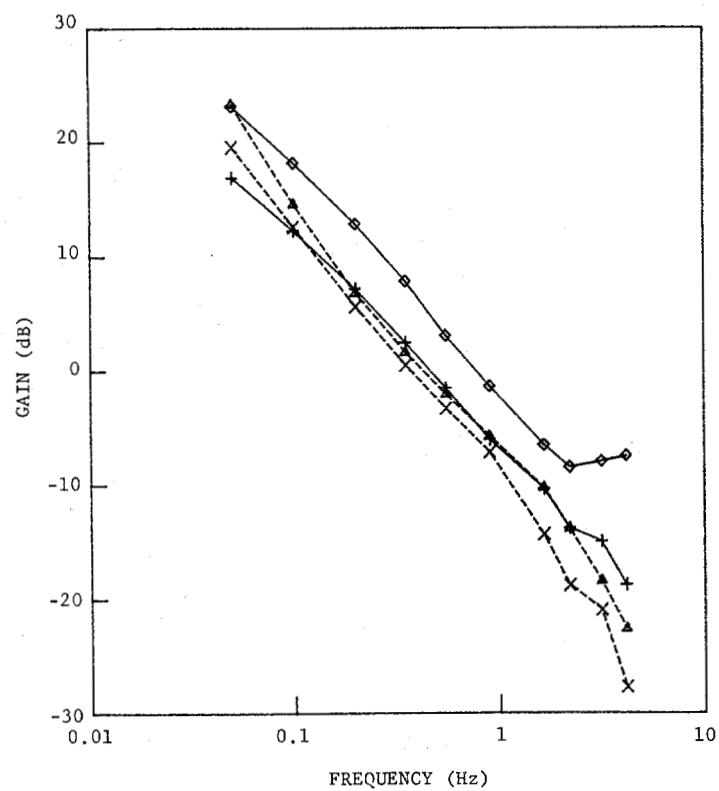


(a)

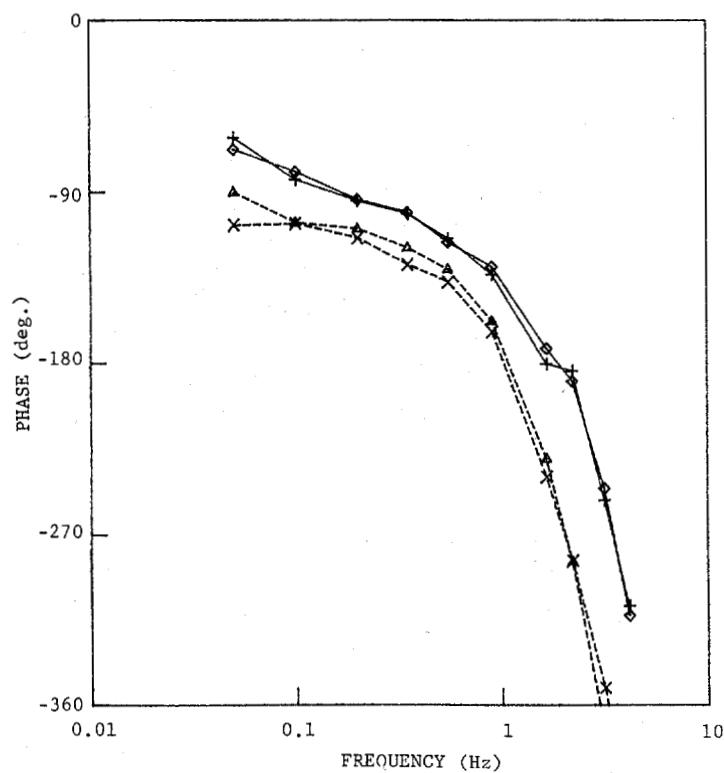


(b)

Fig. 8. Bode plots of closed-loop transfer functions from target input to system output for position pursuit control (—, \diamond), position compensatory (—, +), rate pursuit (---, \triangle), and rate compensatory (---, \times). (a) Bode gain plot, (b) Bode phase plot.



(a)



(b)

Fig. 9. Bode plots of open-loop transfer functions from position error to system output for position pursuit (—, \diamond), position compensatory (—, +), rate pursuit (---, \triangle), and rate compensatory control (---, \times). For pursuit tracking, feedforward components are included in open-loop transfer function. (a) Bode gain plot. (b) Bode phase plot.

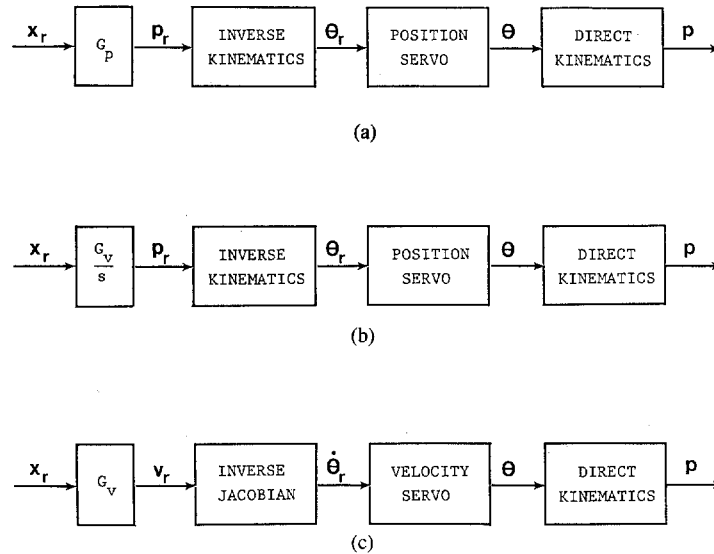


Fig. 10. Simulation models of three implementation schemes. (a) Position control with position servo. (b) Rate control with position servo. (c) Rate control with rate servo. x_r : joystick displacement input for each axis; p_r : desired manipulator hand position; v_r : desired manipulator hand velocity; θ_r : desired joint angle or sliding for each joint; θ : actual joint angle or sliding; p : actual manipulator hand position.

this poor resolution problem is to use indexing [1], [20]. In the indexed position control mode, the control stick gain is selected so that the full displacement range of the control stick covers only a small portion of the manipulator work space. Large movements of the manipulator hand can be made by successive uses of an indexing trigger mounted on the control stick. Note, however, that rate control can inherently provide any higher degree of resolution by mere change of control stick gain without use of indexing.

III. EFFECTS OF MANIPULATOR SYSTEM DYNAMICS

So far ideal position and rate control have been considered by assuming that the manipulator system response is very fast relative to the human operator's control dynamics. In this section, effects of manipulator system dynamics on performance in the position and rate control modes are investigated.

A. Implementation of Position and Rate Control

A simple three-degree-of-freedom cylindrical manipulator is simulated for the pick-and-place task. In general, the computation of dynamic motion of a manipulator requires knowledge of kinematics and dynamics of the manipulator, an actuator model, and the control law pertaining to the actuator servo system. The modeling of a manipulator, permanent-magnet dc motors, and position servos can be found elsewhere [21], [22].

In position control, joystick displacements indicate the desired manipulator end effector position in robot base Cartesian coordinates. To implement position control, we assume that each of the manipulator joints is controlled by a position servo. The simulation model of the position-controlled manipulator system is shown in Fig. 10(a). First joystick displacements are converted into the desired manipulator hand position with a joystick gain G_p for each axis. The desired position is then transformed to the desired joint angle or sliding for each joint by performing the inverse kinematic

position transformation. The model of a position servo with a speed limit is shown in Fig. 11(a). This model is arranged so that it has a unity-gain negative feedback velocity loop with a nonlinear velocity limiter placed in front of the velocity loop. Note that the overall transfer function of the position servo becomes $a^2/(s + a)^2$ without the speed limit. The natural frequency of the manipulator system is given by $\omega_n = a$ rad/s or $f_n = a/2\pi$ Hz. Real-time computer simulation of the position servo can be accomplished by using difference equations for the velocity loop $2a/(s + 2a)$ and the integrator $1/s$ in Fig. 11(a). A simulation program that computes the actual joint angle or sliding as the output of a position servo can be written as

$$\begin{aligned}
 v_r &= (q_r - q) * a/2.0; & \text{amplification of position error} \\
 \text{if } (v_r > v_m) v_r &= v_m; & \text{speed limit} \\
 \text{if } (v_r < -v_m) v_r &= -v_m; \\
 v &= b * v + c * v_r; & \text{velocity loop } 2a/(s + 2a) \\
 q &= q + T * v; & \text{integrator } 1/s.
 \end{aligned}$$

Coefficients a , b , and c are precomputed as $a = 2\pi f_n$, $b = e^{-2aT}$, and $c = 1.0 - b$, where T is the sampling period. In our experiments, T was 50 ms or the sampling frequency was 20 Hz. After computation of the joint angle or sliding for each joint, the manipulator hand position can be obtained by employing direct kinematic equations.

In rate control, joystick displacements indicate the desired manipulator hand velocity in robot base Cartesian coordinates. Rate control can be implemented by using either a position servo or a rate servo for each joint. Simulation models for these two methods are shown in Fig. 10(b) and (c), respectively. When a position servo is used for each joint, implementation of rate control is exactly the same as that of position control except that the joystick displacement for each

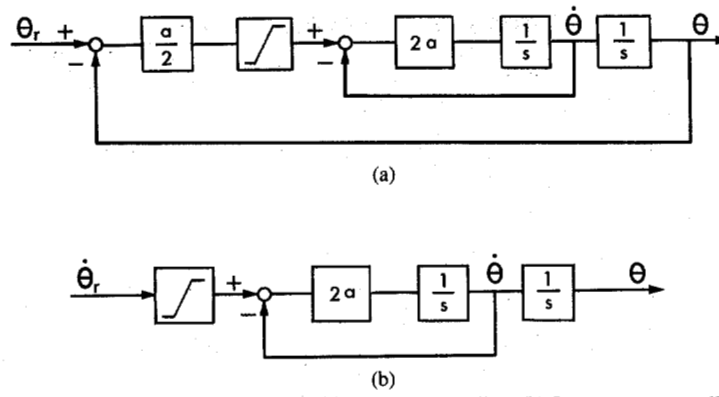


Fig. 11. Block diagrams (a) Position servo controller. (b) Rate servo controller.

axis is integrated before inverse kinematic position transformation. When a velocity servo is used for each joint, this integration is not necessary. As shown in Fig. 10(c), the desired manipulator hand velocity indicated by the joystick displacement for each axis with a joystick gain G_v is directly transformed to the desired velocity of the joint angle or sliding for each joint by employing the inverse kinematic velocity transformation (inverse Jacobian). The desired velocity of the joint angle or sliding for each joint is then applied to the input of each velocity servo. A model of the velocity servo is shown in Fig. 11(b). This model is obtained by removing the position feedback loop from the position servo model of Fig. 11(a). Note that the overall transfer function of the velocity servo becomes $2a/(s + 2a)$ without the speed limit.

B. Effects of Natural Frequency

The effects of the manipulator system dynamics can be studied by varying the natural frequency (f_n) and speed limit ($-V_m$ to $+V_m$). In this section, the effects of the natural frequency of the manipulator system are studied, assuming that there is no speed limit. When $V_m = \text{infinity}$ and if a Cartesian-type manipulator system is used, the overall system transfer function for each axis, from the joystick displacement input to the actual manipulator hand position output, can be obtained by referring to Figs. 10 and 11 as

$$H(s) = G_p a^2 / (s + a)^2 \quad \text{for position control,} \quad (5)$$

$$H(s) = G_v a^2 / s(s + a)^2 \quad \text{for rate control with position servo,} \quad (6)$$

$$H(s) = G_v 2a / s(s + 2a) \quad \text{for rate control with velocity servo.} \quad (7)$$

In our experiments, a cylindrical manipulator system is used, and the dynamics of the three joints cannot be completely decoupled as in the Cartesian manipulator. However, the above equations are still very useful for this discussion as good approximations. When both natural frequency f_n and speed limit V_m approach infinity, the overall system transfer function becomes ideal position or rate control. Namely,

$$H(s) = G_p \quad \text{for position control,} \quad (8)$$

$$H(s) = G_v / s \quad \text{for the two rate controls.} \quad (9)$$

Three-axis pick-and-place tasks were performed with the cylindrical manipulator system for natural frequencies of 0.1, 0.2, 0.4, 0.8, 1.6, 3.2, and 6.4 Hz. Joystick gains were set at $G_p = 2$ for position control, and $G_v = 4$ for the two rate controls as before (see Fig. 2 and Section II-D).

The experimental results in Fig. 12 show that for manipulator natural frequency higher than about 3 Hz, the mean completion time converges to a constant level. In this high natural frequency range, human operator's control dynamics limit the speed of task performance, and a further increase in natural frequency does not improve the task performance speed. In Fig. 12, the convergence level of the mean completion time is approximately 2.8 s for position control, and 4.6 s for the two rate controls. These convergence levels are consistent with the mean completion time results of Fig. 2 for ideal position and rate control.

Fig. 12 also shows that, for natural frequency of the manipulator system lower than about 1 Hz, mean completion time increases significantly. In this low natural frequency range, the manipulator system responds slowly to the human operator's control command, and the sluggishness of the manipulator system limits the speed of the pick-and-place task performance. Equations (5)–(7) show that as the natural frequency approaches 0, position control becomes a^2/s^2 (acceleration control), rate control with velocity servo $2a/s^2$ (also acceleration control), and rate control with position servo a^2/s^3 (jerk control). Since jerk control is one degree higher than acceleration control, rate control with position servo should be the worst in performance at low natural frequencies, which agrees with the results of Fig. 12. Position control should be equivalent in performance to rate control with velocity servo at low natural frequencies, if joystick gains were adjusted such that $G_p a^2 = G_v 2a$. In our experiment, however, joystick gains were fixed for convenience, even though $1 > 2a \gg a^2$ when $a = 0.1$ – 0.2 . Therefore, rate control with velocity servos appeared to perform significantly better than the position control for low natural frequencies in Fig. 12.

When the natural frequency of the manipulator system is low, the task performance is not only slow but also prone to overshoot. This is because it is difficult for the human operator to stop a telemanipulator with slow dynamics quickly and precisely. Thus, for safe and reliable teleoperations, it is best to design a telemanipulator system so that the natural

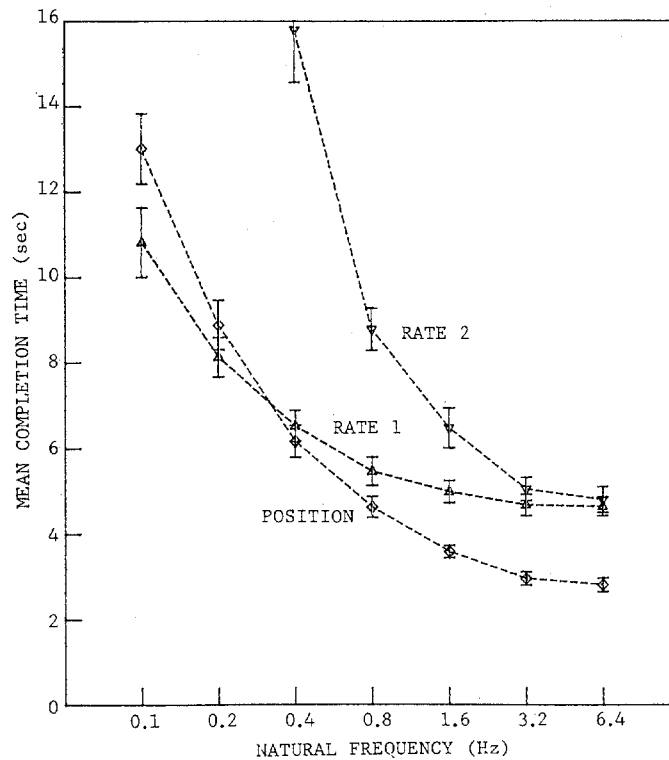


Fig. 12. Effects of natural frequency for position control (◇), rate control with position servo (rate 2, ▽), and rate control with velocity servo (rate 1, △).

frequency for each joint is above 3 Hz, if possible. The structural resonance frequency, however, can be a limiting factor, especially when the manipulator system is large. To prevent excessive mechanical vibrations, the natural frequency of the manipulator system for each joint should not be higher than half of the structural resonance frequency for the corresponding joint. The natural frequency of the SRMS in a straight arm configuration is approximately 0.35 Hz with no load and 0.027 Hz with a 32 000-lb payload attached [23].

C. Effects of Speed Limit

In this section, the effects of the speed limit of the manipulator system are investigated, assuming that the natural frequency of the manipulator system is designed to be sufficiently high. With $f_n = 5$ Hz, three-axis pick-and-place tasks were performed for speed limits $V_m = 0.1, 0.2, 0.4, 0.8, 1.6, 3.2,$ and 6.4 units/s for each joint. In this experiment, the range of the joint angle or sliding is assumed to be ± 1 unit for each joint. In rate control, besides V_m , joystick gain G_v also limits the speed of the manipulator hand movement to G_v units/s for each axis. Joystick gains used were $G_p = 2$ for position control, $G_v = 4$ for rate control with velocity servo, and $G_v = V_m$ for rate control with position servo. The use of the condition $G_v = V_m$, instead of $G_v = 4$, was necessary for rate control with position servo, because when $G_v \gg V_m$, the integrator output is prone to reach a saturation limit during the performance of the control, resulting in excessive overshoots. If the manipulator system is more complicated than the cylindrical manipulator, a more complicated constraint based on the inverse Jacobian, rather

than a simple constraint $G_v = V_m$, would be required to avoid excessive overshoots for rate control with position servo.

Experimental results are shown in Fig. 13. When the speed limit is high, or $V_m > 4$ units/s, the mean completion times for position and rate control approach those of ideal position and rate control in Fig. 2. However, when the speed limit V_m gets below about 1 unit/s, the sluggishness of the manipulator system limits the human operator's pick-and-place performance, and the mean completion time becomes longer for both position and rate control. Mean completion times for position and rate control are virtually the same for low speed limits in Fig. 13. This shows that when the speed limit is very low, position control does not provide any significant advantage over rate control. This result demonstrates that performance with rate control will be at least as good as that of indexed position control in controlling a slow wide-work-space manipulator, because rate control can maintain high resolution for the wide-work-space manipulator without use of an indexing button, while indexed position control requires the use of an indexing button. However, the amount of advantage is not investigated in this paper. The SRMS is a typical example of a slow wide-work-space manipulator. The SRMS is 50 ft 3 in (15.762 m) in length, and it takes approximately 40 s for the SRMS to bend its elbow 90° with full payload, and approximately 4 s with no payload [4].

IV. DISCUSSION

All of the experimental results demonstrated that performance with ideal position control was better than with ideal rate control regardless of joystick type (displacement or force),

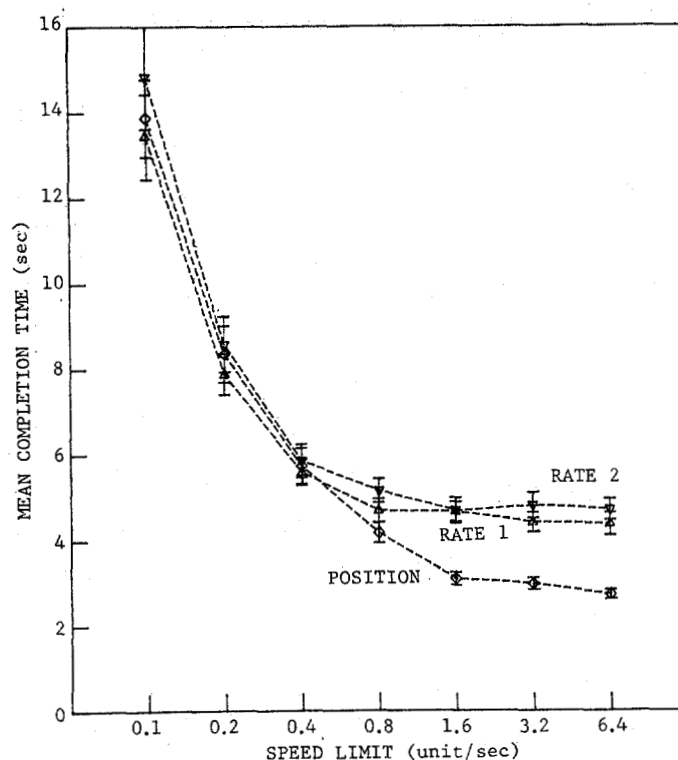


Fig. 13. Effects of speed limit for position control (\diamond), rate control with position servo (rate 2, ∇), and rate control with velocity servo (rate 1, \triangle).

display mode (pursuit or compensatory), or task (pick-and-place or tracking). However, both the pick-and-place and manual tracking experiments implicitly assumed that the telemanipulation or tracking work space was small or at least not very large compared to the joystick control space by allowing the task to be performed with a display that showed the entire work space in one screen. When the telemanipulator has a wide work space, position control requires indexing (i.e., redefinition of the origin of joystick coordinates) to provide acceptable control resolution, whereas rate control does not need indexing. Thus our results demonstrating superiority of position control may apply only to small work space telemanipulation tasks or proximity operations.

When the manipulator system is not sufficiently fast, dynamics deviate from ideal position and rate control. The effects of manipulator system dynamics on position and rate control were investigated in this paper by assuming that manipulator system dynamics depend mainly upon two parameters, the natural frequency and the speed limit of the manipulator system. Both the natural frequency and the speed limit experiments showed that, when the manipulator system was slow due to low natural frequency or low speed limit, sluggishness of the manipulator system limited the speed of pick-and-place performance, and the superiority of position control disappeared. This result strongly suggests that performance with rate control will be at least as good as with indexed position control in controlling slow wide-work-space telemanipulators.

Two implementations of rate control were considered in the paper. The experimental results showed that rate control with velocity servo was superior to rate control with position servo,

especially when the natural frequency of the manipulator system is low. This was because the dynamics of rate control with velocity servo approached acceleration control for low natural frequency, while the dynamics of rate control with position servo approached jerk control, one degree higher.

V. CONCLUSION

Pick-and-place experiments showed that ideal position control performance was better than ideal rate control regardless of joystick type or display mode, when the manipulation work space was small or comparable to the human operator's control space. The manual tracking experiment with two different display modes supported the above result. Therefore, when a telemanipulator has a sufficiently small work space, the use of position control is recommended. Applications of small-work-space telemanipulators can be found in nuclear reactor teleoperators, surgical micromanipulators, and a small dexterous telerobotic hand attached to the end of the main telemanipulator. Position control can also be employed in conjunction with force reflection in proximity operations.

Effects of manipulator system dynamics on the performance of position and rate control were also investigated in this paper. For manipulator natural frequency higher than about 3 Hz, the speed of the pick-and-place task performance was limited by the human operator's dynamics, and further increase in natural frequency did not improve the performance speed. For natural frequency lower than about 1 Hz, the speed was limited by the sluggishness of the manipulator system. When the manipulator system was very slow, superiority of position control disappeared. Considering that position control requires indexing in controlling wide-work-space telemanipu-

lators, while rate control does not need indexing, rate control is recommended for slow wide-work-space telemanipulators.

REFERENCES

- [1] E. G. Johnsen and W. R. Corliss, *Human Factors Applications in Teleoperator Design and Operation*. New York: Wiley-Interscience, 1971.
- [2] E. Heer, *Remotely Manned Systems: Exploration and Operation in Space*. Pasadena, CA: California Inst. Technol., 1973.
- [3] D. E. Whitney, "Resolved motion rate control of manipulators and human prostheses," *IEEE Trans. Man-Mach. Syst.*, vol. MMS-10, pp. 47-53, 1969.
- [4] Rockwell International, STS-7 Press Information, June 1983.
- [5] L. M. Jenkins, "Telerobotic work system—Space robotic application," in *Proc. IEEE Int. Conf. Robotics and Automation*, vol. 2, pp. 804-806, 1986.
- [6] D. P. Millen, "An evaluation of resolved motion rate control for remote manipulators," Charles Stark Draper Lab., 1973.
- [7] J. L. Nevins, T. B. Sheridan, D. E. Whitney, and A. E. Woodin, "The multi-moded remote manipulator system," in *Remotely Manned Systems*, E. Herr, Ed., Pasadena, CA: California Inst. Technol., 1973, pp. 173-187.
- [8] D. R. Wilt, D. L. Pieper, A. S. Frank, and G. G. Glenn, "An evaluation of control modes in high gain manipulator systems," *Mechanism and Machine Theory*, vol. 12, no. 5, pp. 373-386, 1977.
- [9] W. S. Kim, F. Tendick, and L. Stark, "Visual enhancements in pick-and-place tasks: Human operators controlling a simulated cylindrical manipulator," this issue, pp. 418-425.
- [10] S. B. Brodie and C. H. Johnson, "Preliminary design and simulations of a shuttle-attached manipulator system," in *Remotely Manned Systems*, E. Herr, Ed., Pasadena, CA: California Inst. Technol., 1973, pp. 105-118.
- [11] D. McRuer, D. Graham, E. Krendel, and W. Reisener, "Human pilot dynamics in compensatory systems: Theory, models, and experiments with controlled elements and forcing function variations," US Air Force AFFDL-TR-65-15, 1965.
- [12] L. R. Young, "On adaptive manual control," *IEEE Trans. Man-Mach. Syst.*, vol. MMS-10, pp. 292-331, 1969.
- [13] C. R. Kelley, *Manual and Automatic Control*. New York: Wiley, 1968.
- [14] E. C. Poulton, "Bias in experimental comparisons between equipment due to the order of testing," *IEEE Trans. Man-Mach. Syst.*, vol. MMS-10, pp. 332-344, 1969.
- [15] D. McRuer, "Human dynamics in man-machine systems," *Automatica*, vol. 16, no. 3, pp. 237-253, 1980.
- [16] T. B. Sheridan and W. R. Ferrell, *Man-Machine Systems: Information, Control, and Decision Models of Human Performance*. Cambridge, MA: MIT Press, 1974.
- [17] L. Stark, *Neurological Control Systems: Studies in Bioengineering*. New York: Plenum, 1968.
- [18] A. K. Bejczy, "Sensors, controls, and man-machine interface for advanced teleoperation," *Science*, vol. 208, no. 4450, pp. 1327-1335, 1980.
- [19] C. R. Flatau, "The manipulator as a means of extending our dexterous capabilities to larger and smaller scales," in *Proc. 21st Conf. Remote Systems Technology*, 1973, pp. 47-50.
- [20] Argonne National Laboratory, "Manipulator systems for space applications," Tech. Rep., Argonne, 1967.
- [21] R. P. Paul, *Robot Manipulators: Mathematics, Programming, and Control*. Cambridge, MA: MIT Press, 1981.
- [22] J. Y. S. Luh, "Conventional controller design for industrial robots—A tutorial," *IEEE Trans. Syst., Man, Cybern.*, vol. SMC-13, no. 3, pp. 298-316, 1983.
- [23] T. H. Ussher and K. H. Doetsch, "An overview of the shuttle remote manipulator system," in *Proc. Space Shuttle Technical Conf.*, 1983, pp. 892-904, NASA CP-2342.

Won S. Kim (S'84), for a photograph and biography please see page 425 of this issue.

Frank Tendick (S'83), for a photograph and biography please see page 425 of this issue.



Stephen R. Ellis received the A.B. degree in behavioral science from the University of California, Berkeley, and the M.A. and Ph.D. degrees in psychology from McGill University, Montreal, PQ, Canada.

He is a Research Scientist at the NASA Ames Research Center and an Assistant Professor of Physiological Optics at the University of California, Berkeley, School of Optometry. His research interests include cognitive influences on eye movements, picture perception, and human spatial orientation.

Dr. Ellis is a member of the Human Factors Society, the American Association for the Advancement of Science, the American Psychological Society, Sigma Chi, and the Association for Computing Machinery.

Lawrence W. Stark (SM'61-F'70), for a photograph and biography please see page 425 of this issue.